energy&fuels

Biofuels and Biomass

Low temperature deoxidization of lignin and its impact on liquid products from pyrolysis

Yanyang Mei, Shipeng Zhang, Hua Wang, Shuangxi Jing, Ting Hou, and Shusheng Pang

Energy Fuels, **Just Accepted Manuscript** • DOI: 10.1021/acs.energyfuels.0c00202 • Publication Date (Web): 24 Feb 2020

Low temperature deoxidization of lignin and its impact on liquid products from pyrolysis

Yanyang Mei [a, b], Shipeng Zhang [a], Hua Wang [a], Shuangxi Jing [a*], Ting Hou [a], Shusheng Pang [c, a]*

[a] *School of Mechanical and Power Engineering, Henan Polytechnic University, Jiaozuo 454003, Henan, PR China*

[b] *State Key Laboratory of Coal Combustion, Huazhong University of Science and Technology, Wuhan 430074, PR China*

[c] *Department of Chemical and Process Engineering, University of Canterbury, Christchurch 8025, New Zealand*

***Corresponding Author**

Email addresses: wanghua@hpu.edu.cn (*Hua Wang*), jsx@hpu.edu.cn (*Shuangxi Jing*)

Abstract: In this study, low temperature deoxidization of lignin at temperature range of 200~390°C as a pretreatment method had been exploited to gain high quality pyrolysis products. A two-dimensional infrared correlation spectroscopy (2D-PCIS) was used to analyze the evolution of the functional groups of lignin in the process of low temperature deoxidization, and the deoxidized samples were pyrolysed in the pyrolysis gas chromatography mass spectrometry (Py-GC/MS). The results of 2D-PCIS showed that the decomposition of the lignin was accelerated from 320 °C and which was dominated by the elimination reaction. Notably, aromatization reaction was intensified at 350 °C, whereas the structure of lilac aromatic ring was more stable than the guaiac aromatic. It was also found that the alcohol hydroxyl group was significantly removed, and due to this removal other functional groups also underwent changes during the deoxidization. The results from Py-GC/MS experiments showed that deoxidization treatment at lower than 230 °C had insignificant effect on the pyrolysis products. However, when the deoxidization temperature was at 230°C and above, the oxygen-containing compounds in the pyrolysis liquid products (mainly phenols) decreased significantly, and when the deoxidization temperature was above 290 °C, hydrocarbons were the main compounds in the pyrolysis liquid product.

Keywords: Lignin; Pretreatment; Deoxidization; 2D-PCIS; Pyrolysis

1. Introduction

Fast pyrolysis was a thermochemical technique which can convert biomass to liquid fuel (bio-oil) [1]. Specifically, bio-oil was a highly complex mixture of water and oxygenated species such as organic acids, carbohydrates, aldehydes, ketones which

originated from the degradation of cellulose, hemicellulose, and lignin [2]. Due to the extremely complex composition and high content of oxygenated compounds, the bio-oil must be upgraded and refined in centralized bio-refineries which converted the bio-oil into liquid fuels or chemicals [3]. However, the cost of such upgrading and refining process was rather high. Therefore, deoxidization pretreatment of biomass was necessary to reduce the complexity and oxygenated compounds in the bio-oil [4].

Torrefaction had attracted noticeable interest among the pretreatment technologies to remove some volatiles and to reduce oxygen content in the biomass [5-7], and thus to improve the quality of bio-oil [8, 9]. Boateng et al. [10] had confirmed that torrefaction caused low bio-oil yield because some oxygen-containing compounds were removed, whereas the bio-oil from pyrolysis of torrefied biomass exhibited some advantages, such as low acidity content. Ukaew et al. [11] had investigated the effects of torrefaction temperatures in the range of 225-275°C on the yield and quality of bio-oil from fast pyrolysis. After torrefaction, the yield of bio-oil from pyrolysis was even reduced to approximately a quarter compared with that of raw biomass. Correspondingly, the water yield was reduced from 1.6 wt. % for pyrolysis of the raw biomass to 0.2 wt. % for the pyrolysis of torrefied biomass at torrefaction temperature of 275°C. However, Liaw et al. [12] reported that the effects of torrefaction pretreatment at temperatures below 270 °C was not significant on the liquid product yields, whereas when the temperature is above 300 °C, the yield of lignin-derived monomers containing methoxy groups decreased sharply, while that of methanol increased. Xiao et al. [13] pointed out that the temperature range of torrefaction was too narrow to

remove as much oxygen as possible. Wang et al. [14] also showed that although torrefaction could reduce the oxygen content of the compounds in the subsequent pyrolysis oil, which could not reduce the types of compounds. Moreover, Yan et al. [15] concluded that high biochar yield also could be achieved even after torrefaction treatment at 300 °C. In view of the above, method of deoxidization pretreatment at a wider temperature was necessary and feasible. In addition, fundamental analysis was also needed to better understand the mechanics of biomass deoxidization and its impact on the subsequent pyrolysis products.

In previous studies, the structural evolution of biomass to biochar during pyrolysis and its impact on the subsequent thermal chemical utilization had been investigated. Fatehi et al. [16] established a comprehensive model to describe the structure evolution of biochar and analyzed the effect of multi-pore structure on biochar reactivity during gasification. Keown et al. [17] also analyzed the structural evolution of biochar during gasification and pointed out that temperature had an important effect on the structure and reactivity of biochar. Fu et al. [18] investigated the structural evolution of char produced by pyrolysis at different temperatures and found that pore opening (ascribed to the removal of volatile matter) was apparent below 500 °C, whereas the biochar shrinkage occurred above 500 °C. Burhenne et al. [19] investigated the influence of initial water content in biomass and operation temperature on the structure and reactivity of pyrolysis char. They found that the char surface area and the reactivity in CO_2 were significantly decreased with increasing pyrolysis temperature, whereas wood water content exhibited no obvious influence. In

our previous study [20], the influences of the biochar structural evolution on the contents and chemical composition of liquid product in pyrolysis of cellulose was investigated. However, the structural evolution of lignin and its impact on the pyrolysis liquid products were not discussed. It was known that the lignin was one of the most significant components in lignocellulosic biomass, and in some biomass species, its content was just after the cellulose [21].

In this study, deoxidization of lignin was investigated at a broad range of temperatures from 200 to 390˚C in a lab-scale fixed bed, and two-dimensional infrared correlation spectroscopy (2D-PCIS) was used to analysis the structural evolution. The deoxidized samples were subsequently pyrolysed by gas chromatography/ mass spectrometry (Py-GC/MS). In this way the effects of lignin deoxidization on the yields and quality of pyrolysis were analysed.

2. Material and Methods

2.1 Lignin sample

The alkali lignin sample provided by Sigma-Aldrich Co., Ltd (Brown powder, particle size = 20 μm, pH=10.5) was dried at 105 °C for 24 h prior to low temperature deoxidization. The proximate and ultimate analyses and the high heat value of raw and deoxidized samples were performed in the previous study [22].

2.2 Experiment of low temperature deoxidization

Deoxidization treatment of the lignin sample was conducted in a lab-scale tube furnace. The experimental method and parameter selection were the same as reported in the previous study for pretreatment of biomass [22].

2.3 Py-GC/MS analysis

Pyrolysis and measurements were performed using a CDS Pyroprobe 5200 pyrolyzer (Chemical Data Systems) and an Agilent 7890A series gas chromatograph equipped with an HP5975 MS detector. Samples of ~0.3 mg weight were introduced into the pyrojector and pyrolyzed at 550 °C, and the obtained products were identified by comparison with the NIST mass spectral data library [23, 24].

2.4 Data processing of solid samples

The mass yields of liquid, gas and solid residues were calculated on a dry basis (d), and defined as follows [25]:

$$\text{Mass yield of solid product } (Y_{sm}) = \frac{\text{Mass(d) of solid product}}{\text{Mass(d) of raw sample}} \times 100\% \cdots\cdots\cdots (1)$$

$$\text{Mass yield of gas product } (Y_{gm}) = \frac{\text{Mass(d) of gas product}}{\text{Mass(d) of raw sample}} \times 100\% \cdots\cdots\cdots (2)$$

$$\text{Mass yield of liquid product } (Y_{lm}) = (1 - Y_{sm} - Y_{gm}) \times 100\% \cdots\cdots\cdots (3)$$

3. Results and Discussion

3.1 Mass yields from low temperature deoxidized lignin

Fig. 1 showed the mass yields of tristate outcome of lignin under different deoxidized temperatures. With temperature increasing, the lignin was decomposed slowly, which was mainly attributed to the fact that the decomposition of unstable groups on aliphatic hydrocarbon branched chains. At the same time, the gas and liquid yields had steadily increased respectively. However, due to the high thermal stability of lignin, its solid yield was still 68.32% at 390 °C. These results indicated that lignin pyrolysis occured over a wide range of temperatures, which was consistent with

previous results [26-28].

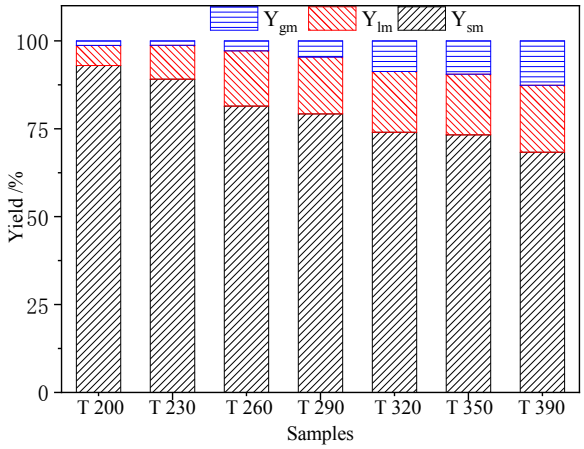

Fig. 1 The pretreatment yields of deoxidized lignin including tri-state outcome. (T200 represents the pretreated lignin at 200 °C).

3.2 Investigation of functional group evolution by FTIR 2D-PCIS

The FTIR atlas for raw and low temperature deoxidized lignin was reported in the previous study [22]. However, due to the low resolution and obvious peak overlap, traditional spectra could not accurately describe the changes of specific peaks and reveal important information about the surface functions of solid residues. Alternatively, the 2D-PCIS method could enhance the resolution of spectra obtained by traditional ways and solved these problems [29]. Therefore, in the present study the 2D-PCIS method was used to extract further information of spectroscopic data.

Fig. 2 showed synchronous and asynchronous 2D correlation spectra in the region of 2750–3750cm^{-1}. Notably, two auto peaks during low temperature deoxidization could be observed, with the stronger one at ~3415cm^{-1} belonging to alcoholic hydroxyl associated with H-bonds (in the same side chain of fatty). The weaker one at ~2924cm^{-1} was the vibration absorption of methylene groups, which reflected that the former bond was more sensitive to temperature and the reaction intensity of methylene groups were weak during low-temperature deoxidization. The

existence of positive cross-peak Φ (3350, 2900) in the synchronous spectrum indicated that there was an interaction between alcoholic hydroxyl and methylene group, and the reaction of alcoholic hydroxyl was earlier than methylene. A number of positive cross-peaks (e.g., Ψ(3415,2816)、Ψ(3415,2877)、Ψ(3415,3165)、Ψ(3415,3611)) were observed in the asynchronous 2D correlation spectrum. The bands at 2816, 2877, 3165, and 3611 cm^{-1} were ascribed to symmetrical stretching vibration of methyl groups in aromatic rings, vibration absorption of methyl groups of fatty hydrocarbon, intermolecular hydrogen bonds between diphenols and other phenolic groups, hydroxyl groups of benzyl, respectively. As shown in synchronous spectra, these cross peaks were all positive values, which indicated that alcoholic hydroxyl reacts first and all other functional groups were related to it.

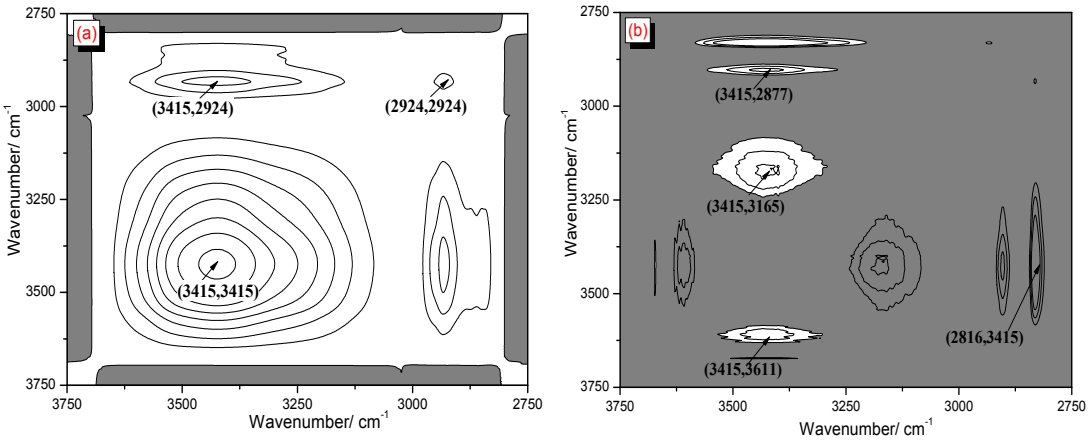

Fig.2 Synchronous (a) and asynchronous (b) 2D correlation spectra of raw and low temperature deoxidized lignin in the range of 2750–3750cm^{-1}. Light gray and white areas indicated negative and positive correlation values, respectively.

Fig. 3 showed synchronous and asynchronous 2D correlation spectra in the region of 1850–850 cm^{-1}. It could be seen from the Fig. 3 that there were many characteristic absorption peaks related to the structure of benzene ring and aliphatic hydrocarbon branched chain, and five auto peaks at 1596, 1506, 1217, 1138, and

1042cm^{-1} were observed. Among them, 1596cm^{-1} and 1506cm^{-1} were the characteristic absorption peaks of the aromatic ring skeleton of lignin, 1217cm^{-1} represented the alkyl ether bond on the aliphatic hydrocarbon branch chain, 1138cm^{-1} was the C-H deformation vibration absorption peak in the aromatic nucleus plane of guaiacol, and 1042cm^{-1} belonged to the vibration absorption peak of C-H in guaiacol aromatic ring together with C-O in aliphatic hydrocarbon primary alcohol hydroxyl [30-33]. It could be also seen that 1042cm^{-1} had cross peaks with many other functional groups, such as 1596cm^{-1}, 1506cm^{-1}, 1217cm^{-1} and 1448cm^{-1} (C=C stretching vibration of the benzene ring skeleton of aromatic compounds), indicating that the reaction of aromatic rings was the main part during low-temperature deoxidization. And these cross peaks were all positive values, indicating that they had the same trend of change with temperature.

Several negative cross-peaks in asynchronous 2D correlation spectrum were also formed at 1117cm^{-1} and other functional groups such as 1042cm^{-1}, 1138cm^{-1}, 1217cm^{-1}, 1265cm^{-1}, 1506cm^{-1}, respectively. According to Noda's rules [29], the spectral change sequence was derived as 1042/ 1138/ 1265/ 1506cm^{-1} > 1217cm^{-1} > 1117cm^{-1}, which indicated that the structure of lilac aromatic ring was more stable than the guaiac aromatic.

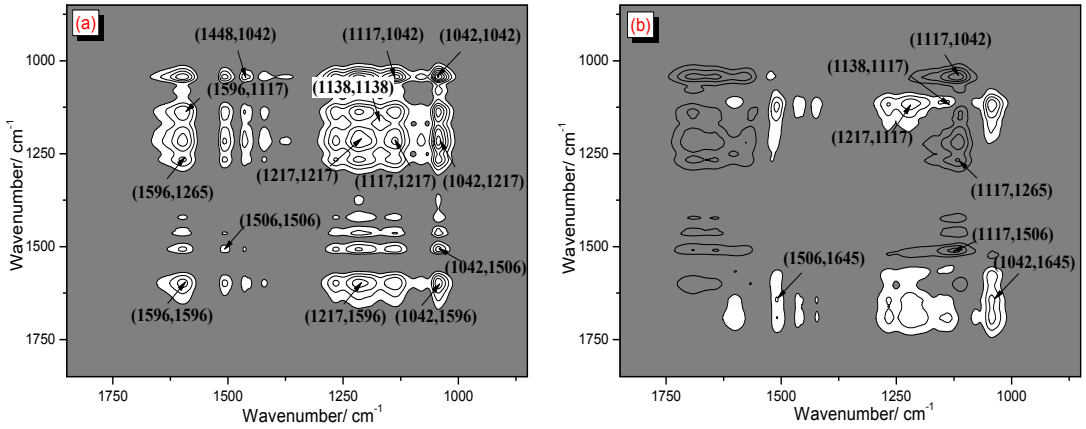

Fig. 3 Synchronous (a) and asynchronous (b) 2D correlation spectra of raw and low temperature deoxidized lignin in the range of 1850–850 cm^{-1}.

Fig. 4 showed the variation in the relative signal intensities of different groups during the low-temperature deoxidization of lignin. From Fig. 4, it was clearly seen that the absorption peak intensity of each functional group showed a decreasing trend with increasing temperature, which indicated that most of the low-temperature deoxidization process of lignin was removal or elimination reaction. However, there were both elimination and formation reactions for cellulose [20], which was mainly due to their different thermal stability. The structure of lignin unit was mostly ether bond and C-C bond, which was very stable and produced less molecular fragments in the low temperature deoxidization process, so it weakened the secondary reaction. In addition, it was also interesting to note that the peak absorption intensity of functional groups at 200 °C was lower than that at 100, 230 and 260 °C, which was mainly because the decomposition reaction at 200 °C was not sufficient and produced fewer molecular fragments, so there were no more secondary reactions. However, when the temperature higher than 260 °C, the decomposition reaction was more intense and the speed of recombination reaction was far lower than the decomposition reaction, so the

intensity of each absorption peak was reduced. The inflection points at 350 °C of 1448 cm^{-1} (aromatic hydrocarbons benzene ring skeleton of C = C stretching vibration) and 1506 cm^{-1} (lignin characteristic absorption peaks of the aromatic ring skeleton) testified that there was a certain competitive relationship between them, and the former indicated that the aromatization reaction was accelerated at 350 °C and the growth rate of aromatics was higher than the removal. The latter showed that the formation of new aromatic rings could inhibit the removal of lignin aromatic rings. The intensity of methyl on aromatic ring (2816 cm^{-1}) showed little change within the temperature range (200–290 °C), indicating that the efficiency of methyl removal was not obvious at the lower deoxidization temperature.

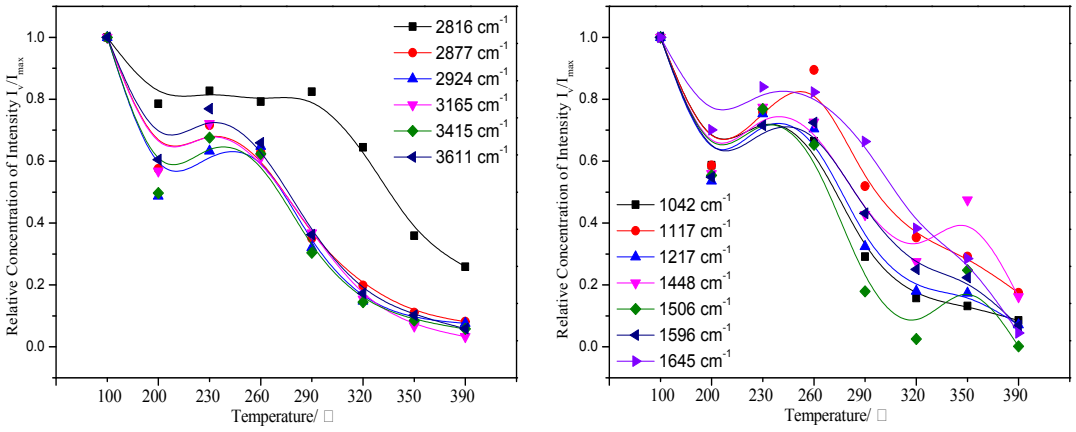

Fig. 4 Variation in the relative intensities (I_v/I_{max} = peak intensity at a given temperature/maximum peak intensity) of peaks observed in synchronous and asynchronous 2D correlation spectra of raw and deoxidized lignin.

3. 3 Analysis of Py-GC/MS Results

Fig. 5 showed the total and distribution of organic products from pyrolysis of lignin which was deoxidized at different temperatures from 200°C (T200) to 390°C (T390). The pyrolysis was performed at Py-GC/MS at 550°C. The results in Fig.5 revealed that the total organic components were decreased slowly with the increase of

deoxidization temperature, and phenols were the most abundant products of the raw lignin pyrolysis, which were mainly generated by the breaking of aryl glycerol- β-aryl ether bonds [28, 34, 35]. When the temperature of deoxidation was over 230 °C, phenolic products decreased rapidly, which was mainly due to hydroxyl removal and benzene ring opening. There were almost no alcohols and acids in the pyrolysis products. The highest aldehyde yield was observed at deoxidization temperature of 230°C, whereas hardly any aldehydes were formed at deoxidization temperatures above 290°C. It was also found that deoxidization at the range of torrefaction temperature (200–290°C) had no effect on ketone products of lignin pyrolysis, whereas at higher temperatures (320–390°C), there were no ketone products.

Fig. 5 also demonstrated that few chain hydrocarbons output in the pyrolysis of raw and treated lignin with low temperature (200–290 ° C). However, the yield of chain hydrocarbon products was increased rapidly in the samples deoxidized at temperatures of 320, 350 and 390°C, which was related to the ring-opening reaction of lignin at higher deoxidation temperature. In addition, relatively more aromatics products were produced in raw lignin pyrolysis, because lignin was a complex natural polymer with phenylpropane group structural unit, and the ether bonds between phenylpropane groups tended to break to form more aromatic compounds. With increasing pretreatment temperature, the content of aromatics in the pyrolysis liquid products gradually increased and the highest yield was observed for sample treated at 320 °C, which was up to 4.3 times of that from pyrolysis of the raw sample. With further increase in the deoxidization temperature, the output was decreased, and at

deoxidization temperature of 390°C, this was only 2.1 times of that from pyrolysis of the raw sample. This finding was ascribed to the enrichment of lignin in the process of low-temperature deoxidation, and the maximum enrichment effect was achieved at 320 °C. It also indicated that the decomposition of lignin was accelerated from 320 °C.

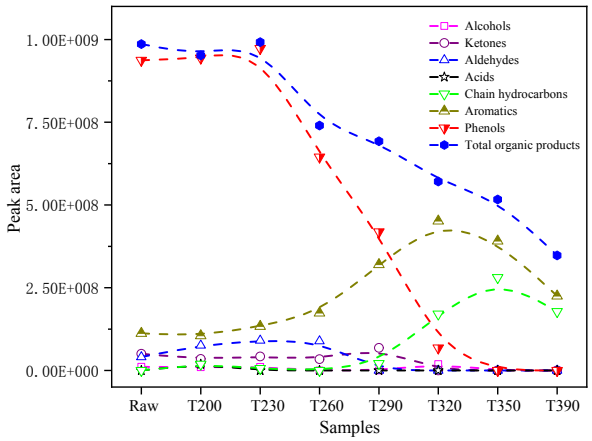

Fig. 5 Total and distribution of organic products of per mg sample after pyrolysis of the oxidized lignin.

3.4 Formation of typical organic products and chemical pathways

Table 1 presented the main components and contents of bio-oil from lignin pyrolysis, revealing that the main products from pyrolysis of the raw lignin were 2-methoxyphenol, 2-methoxy-4-vinylphenol and 2-methoxy-4-methylphenol, which was related to the presence of more guaiac-based propane monomers in lignin. Pyrolysis of pretreated samples which deoxidization at 200, 230, 260 and 290°C produced liquid product with similar composition to that of the raw sample. However, the liquid product from pyrolysis of deoxidized samples at 260 and 290°C did not have 2-methoxy-4-vinylphenol, but had d-limonene and toluene, which were the main products from pyrolysis of T320, T350 and T390 samples. The overlap of the main

products in the T260 and T290 samples indicated that the structure of lignin was not a sudden change but a slow decomposition during the low temperature deoxidization. And the disappearance of 2-methoxyphenol in pyrolysis products promised that aromatization was intensified and char was generated.

Table 1 The main components and contents of bio-oil.

Compound	Peak area percentage (%)							
	Raw	T200	T230	T260	T290	T320	T350	T390
2-methoxyphenol	38.12	35.79	34.82	20.31	28.17	–	–	–
2-methoxy-4-vinylphenol	6.62	7.64	6.32	–	–	–	–	–
2-methoxy-4-methylphenol	5.75	5.77	5.83	6.05	6.83	–	–	–
d-limonene	–	–	–	4.17	19.55	42.40	44.26	42.35
toluene	–	–	–	1.44	4.41	10.51	7.30	3.78

Fig. 6 showed the suggested chemical pathways for the formation of typical lignin pyrolysis products. Pathway 1 represented the formation of 2-methoxy-4-vinylphenol, which were mainly formed by the breakdown of the β-O-4 ether bond in guaiac-based branched chain and the hydroxyl removal at the α position. The formation of 2-methoxy-4-methylphenol was mainly caused by the break of carbon bond between α and β in guaiac-based branch chain (as showed in pathway 3), and torrefaction pretreatment was beneficial to its formation[36]. The 2-methoxyphenol in pathway 6 originated from the removal of branch chains of guaiac-based units[37].

The formation of toluene was related to the dehydroxylation of cresol, such as pathways 5 and 8 [38, 39]. As for d-limonene, its formation path was relatively complex, which might be the product of recombination and synthesis of small molecule compounds after ether bond breaking, or formed by opening and recombination of benzene ring.

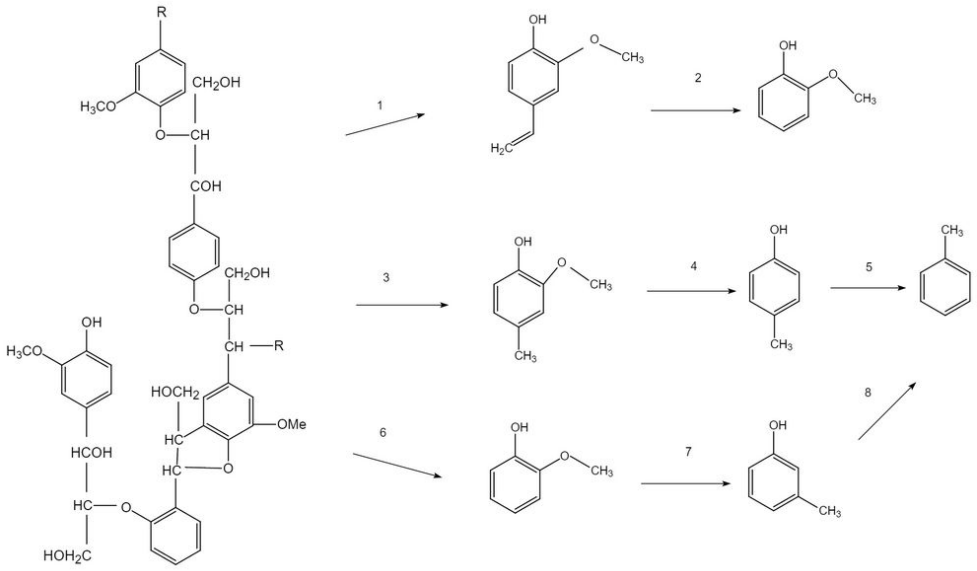

Fig.6 Chemical pathways proposed for the formation of typical lignin pyrolysis products.

4. Conclusions

The evolution of functional groups during low-temperature deoxidization of lignin and its impacts on subsequent pyrolytic liquid (bio-oil) products had been investigated in this study. The pathways of typical compounds in bio-oil were also inferred. Lignin had high thermal stability and its solid yield was still 68.32% at 390 °C pretreatment. Meanwhile, the main reaction of low temperature deoxidization of lignin was the removal of alcohol hydroxyl group. However, high-temperature pretreatment could reduce the oxygen content of bio-oil and promoted the composition simplification. After pretreatment at 320 °C or higher, almost all the

components of bio-oil were hydrocarbons.

Acknowledgements

This study is supported by Henan Postdoctoral Foundation (1902037), Science and Technology Research Project of Henan Province (182102310888), Fundamental Research Funds for the Universities of Henan Province (NSFRF180303), Funding Scheme of the Young Key Teachers of the Higher Education University in Henan (2017GGJS050) and National Natural Science Foundation of China (U1404520).

References

1. Makkawi, Y.; Yu, X.; Ocone, R., Parametric analysis of biomass fast pyrolysis in a downer fluidized bed reactor. *Renewable Energy* **2019,** 143, 1225-1234.
2. Wang, W.; Li, X.; Ye, D.; Cai, L.; Shi, S. Q., Catalytic pyrolysis of larch sawdust for phenol-rich bio-oil using different catalysts. *Renewable Energy* **2018,** 121, 146-152.
3. Aysu, T.; Fermoso, J.; Sanna, A., Ceria on alumina support for catalytic pyrolysis of Pavlova sp. microalgae to high-quality bio-oils. *Journal of Energy Chemistry* **2017,** 27, 874-882..
4. Mohan, D.; Pittman, C. U.; Steele, P. H., Pyrolysis of Wood/Biomass for Bio-Oil: A Critical Review. *Energy & Fuels* **2006,** 20, (3), 848--889.
5. Dai, L.; Wang, Y.; Liu, Y.; Ruan, R.; He, C.; Yu, Z.; Jiang, L.; Zeng, Z.; Tian, X., Integrated process of lignocellulosic biomass torrefaction and pyrolysis for upgrading bio-oil production: A state-of-the-art review. *Renewable and Sustainable Energy Reviews* **2019,** 107, 20-36.
6. Sukiran, M. A.; Abnisa, F.; Daud, W. M. A. W.; Bakar, N. A.; Loh, S. K., A review of torrefaction of oil palm solid wastes for biofuel production. *Energy Conversion and Management* **2017,** 149, 101-120.
7. Chew, J. J.; Doshi, V., Recent advances in biomass pretreatment–Torrefaction fundamentals and technology. *Renewable and sustainable energy reviews* **2011,** 15, (8), 4212-4222.
8. Van der Stelt, M.; Gerhauser, H.; Kiel, J.; Ptasinski, K., Biomass upgrading by torrefaction for the production of biofuels: a review. *Biomass and Bioenergy* **2011,** 35, (9), 3748-3762.
9. Zheng, Y.; Tao, L.; Yang, X.; Huang, Y.; Liu, C.; Gu, J.; Zheng, Z., Effect of the Torrefaction Temperature on the Structural Properties and Pyrolysis Behavior of Biomas. *Bioresources* **2017,** 12, (2), 3425-3447.
10. Boateng, A.; Mullen, C., Fast pyrolysis of biomass thermally pretreated by torrefaction. *Journal of Analytical and Applied Pyrolysis* **2013,** 100, 95-102.
11. Ukaew, S.; Schoenborn, J.; Klemetsrud, B.; Shonnard, D. R., Effects of torrefaction temperature and acid pretreatment on the yield and quality of fast pyrolysis bio-oil from rice straw. *Journal of Analytical and Applied Pyrolysis* **2018,** 129, 112-122.
12. Liaw, S. S.; Shuai, Z.; Wu, H.; Garcia-Perez, M., Effect of pretreatment temperature on the yield and properties of bio-oils obtained from the auger pyrolysis of Douglas fir wood. *Fuel* **2013,** 103, (1), 672-682.
13. Xiao, R.; Chen, X.; Wang, F.; Yu, G., Pyrolysis pretreatment of biomass for entrained-flow gasification. *Applied Energy* **2010,** 87, (1), 149-155.

14. Wang, X.; Wu, J.; Chen, Y.; Pattiya, A.; Yang, H.; Chen, H., Comparative study of wet and dry torrefaction of corn stalk and the effect on biomass pyrolysis polygeneration. *Bioresource Technology* **2018,** 258, 88-97.

15. Yan, W.; Perez, S.; Sheng, K., Upgrading fuel quality of moso bamboo via low temperature thermochemical treatments: Dry torrefaction and hydrothermal carbonization. *Fuel* **2017,** 196, 473-480.

16. Fatehi, H.; Bai, X. S., Structural evolution of biomass char and its effect on the gasification rate. *Applied Energy* **2017,** 185, 998-1006.

17. Keown, D. M.; Li, X.; Hayashi, J. I.; Li, C. Z., Evolution of biomass char structure during oxidation in O_2 as revealed with FT-Raman spectroscopy. *Fuel Processing Technology* **2008,** 89, (12), 1429-1435.

18. Fu, P.; Hu, S.; Sun, L.; Xiang, J.; Yang, T.; Zhang, A.; Zhang, J., Structural evolution of maize stalk/char particles during pyrolysis. *Bioresource Technology* **2009,** 100, (20), 4877-4883.

19. Burhenne, L.; Damiani, M.; Aicher, T., Effect of feedstock water content and pyrolysis temperature on the structure and reactivity of spruce wood char produced in fixed bed pyrolysis. *Fuel* **2013,** 107, (9), 836-847.

20. Mei, Y.; Yang, Q.; Yang, H.; Li, J.; Zeng, K.; Chen, Y.; Zhang, S.; Chen, H., Impact of cellulose deoxidization temperature on the composition of liquid products obtained by subsequent pyrolysis. *Fuel processing technology* **2019,** 184, 73-79.

21. Bu, Q.; Chen, K.; Xie, W.; Liu, Y.; Cao, M.; Kong, X.; Chu, Q.; Mao, H., Hydrocarbon rich bio-oil production, thermal behavior analysis and kinetic study of microwave-assisted co-pyrolysis of microwave-torrefied lignin with low density polyethylene. *Bioresource technology* **2019,** 291, 121860.

22. Mei, Y.; Yang, Q.; Yang, H.; Lin, G.; Li, J.; Chen, Y.; Zhang, S.; Chen, H., Low temperature deoxidization of biomass and its release characteristics of gas products. *Industrial Crops and Products* **2018,** 123, 142-153.

23. Lu, X. Q.; Hanna, J. V.; Johnson, W. D., Source indicators of humic substances: an elemental composition, solid state 13 C CP/MAS NMR and Py-GC/MS Study. *Applied Geochemistry* **2000,** 15, (7), 1019-1033.

24. Qiang, L.; Zhang, Z. F.; Dong, C. Q.; Zhu, X. F., Catalytic upgrading of biomass fast pyrolysis vapors with nano metal oxides: an analytical Py-GC/MS Study. *Energies* **2010,** 3, (11), 1805-1820.

25. Bridgeman, T.; Jones, J.; Shield, I.; Williams, P., Torrefaction of reed canary grass, wheat straw and willow to enhance solid fuel qualities and combustion properties. *Fuel* **2008,** 87, (6), 844-856.

26. Yang, H.; Yan, R.; Chen, H.; Lee, D. H.; Zheng, C., Characteristics of hemicellulose, cellulose and lignin pyrolysis. *Fuel* **2007,** 86, (12-13), 1781-1788.

27. Huang, Y.; Wei, Z.; Yin, X.; Wu, C., Pyrolytic characteristics of biomass acid hydrolysis residue rich in lignin. *Bioresource Technology* **2012,** 103, (1), 470-476.

28. Huang, Y.; Wei, Z.; Qiu, Z.; Yin, X.; Wu, C., Study on structure and pyrolysis behavior of lignin derived from corncob acid hydrolysis residue. *Journal of Analytical and Applied Pyrolysis* **2012,** 93, (0), 153-159.

29. Noda, I., Two-Dimensional Infrared (2D IR) Spectroscopy: Theory and Applications. *Applied Spectroscopy* **1990,** 44, (4), 550-561.

30. Yan, T.; Xu, Y.; Yu, C., The isolation and characterization of lignin of kenaf fiber. *Journal of Applied Polymer Science* **2009,** 114, (3), 1896-1901.

31. Nada, A.-A. M. A.; El-Sakhawy, M.; Kamel, S. M., Infra-red spectroscopic study of lignins. *Polymer Degradation and Stability* **1998,** 60, (2–3), 247-251.

32. Boeriu, C. G.; Bravo, D.; Gosselink, R. J. A.; van Dam, J. E. G., Characterisation of structure-dependent functional properties of lignin with infrared spectroscopy. *Industrial Crops and Products* **2004,** 20, (2), 205-218.

33. Suhas; Carrott, P. J. M.; Ribeiro Carrott, M. M. L., Lignin – from natural adsorbent to activated carbon: A review. *Bioresource Technology* **2007,** 98, (12), 2301-2312.

34. Guo, X. J.; Wang, S. R.; Wang, K. G.; Luo, Z. Y., Experimental Researches on Milled Wood Lignin Pyrolysis Based on Analysis of Bio-oil. *Chemical Research in Chinese Universities***2011,** 27, (3), 426-430.

35. Kim, J. Y.; Oh, S.; Hwang, H.; Kim, U. J.; Choi, J. W., Structural features and thermal degradation properties of various lignin macromolecules obtained from poplar wood (Populus albaglandulosa). *Polymer Degradation and Stability* **2013,** 98, (9), 1671-1678.

36. Zhang, L.; Li, S.; Li, K.; Zhu, X., Two-step pyrolysis of corncob for value-added chemicals and high quality bio-oil: Effects of pyrolysis temperature and residence time. *Energy conversion and Management* **2018,** 166, 260-267.

37. Pelucchi, M.; Cavallotti, C.; Cuoci, A.; Faravelli, T.; Frassoldati, A.; Ranzi, E., Detailed kinetics of substituted phenolic species in pyrolysis bio-oils. *Reaction Chemistry & Engineering* **2019,** 4, (3), 490-506.

38. Srinivasan, V.; Adhikari, S.; Chattanathan, S. A.; Park, S., Catalytic pyrolysis of torrefied biomass for hydrocarbons production. *Energy & Fuels* **2012,** 26, (12), 7347-7353.

39. Fang, S.; Jiang, L.; Li, P.; Bai, J.; Chang, C., Study on pyrolysis products characteristics of medical waste and fractional condensation of the pyrolysis oil. *Energy,* **2020**, 195, (3),116969.